Journal of
Mechanics of
Materials and Structures

APPLICATION AND DESIGN OF LEAD-CORE BASE ISOLATION FOR REDUCING STRUCTURAL DEMANDS IN SHORT STIFF AND TALL STEEL BUILDINGS AND HIGHWAY BRIDGES SUBJECTED TO NEAR-FIELD GROUND MOTIONS

Thomas L. Attard and Kittinan Dhiradhamvit

Volume 4, Nº 5 May 2009

mathematical sciences publishers

JOURNAL OF MECHANICS OF MATERIALS AND STRUCTURES
Vol. 4, No. 5, 2009

APPLICATION AND DESIGN OF LEAD-CORE BASE ISOLATION FOR REDUCING STRUCTURAL DEMANDS IN SHORT STIFF AND TALL STEEL BUILDINGS AND HIGHWAY BRIDGES SUBJECTED TO NEAR-FIELD GROUND MOTIONS

THOMAS L. ATTARD AND KITTINAN DHIRADHAMVIT

The performance of nonlinear lead-core-rubber base isolators (LCR) to passively control highly nonlinear vibrations in two steel buildings and a prestressed concrete bridge under various ground motion inputs is evaluated. The Bouc and Wen model is used to predict the behavior of the lead-core component of the LCR base isolator. Members of the steel buildings that may have yielded are analyzed according to a highly nonlinear constitutive rule used to model the smooth stiffness degradation in the damaged members. The previously developed constitutive rule analyzes kinematically strain-hardened materials under cyclic conditions. The ability of the LCR to reduce displacement, velocity, and acceleration demands is demonstrated numerically using an algorithm developed herein called BISON (base isolation in nonlinear time history analysis). The performance of the LCR isolation is measured for a two story isolated building excited by the El Centro ground motion, a nonstationary signal, and the Northridge ground motion. An eight-story building exhibiting higher-mode influence is also analyzed, and finally the overpass bridge on Highway 99 in Selma, CA is modeled, outfitted with LCR isolation, and also analyzed. The hysteresis of the force-displacement relationships of the structures and the LCR isolators are analyzed parametrically through two LCR design parameters. The results indicate that with an appropriate tuning of these parameters, which affect the inelastic stiffness of the LCR isolator, an appropriate LCR system may be designed to behave with a stationary-like hysteresis and that can very adequately reduce the structural demands under the various excitations.

1. Introduction

In large civil structures, including highway bridges and buildings, passive energy dissipation systems are preferred over active control systems because of lower cost, less maintenance, and lower power consumption. Seismic base isolation implementation remains one of the most widely used and accepted passive methods used to protect buildings and bridges from potential earthquake hazards. The concept of base isolation focuses on altering a structure's natural frequency away from the dominant frequency components of a seismic event [Kikuchi and Aiken 1997; Furukawa et al. 2005]. Base isolation systems are also used to protect the nonstructural components in buildings, including pipes, electrical wires, and various equipment, which may be found in hospitals and communication centers [Pozo et al. 2006; Matsagar and Jangid 2004], by reducing interstory displacement demands and accelerations through hysteretic energy dissipation [Matsagar and Jangid 2008; Dolce et al. 2007]. Some typical base isolators

Keywords: base isolation, passive control, bridge isolation, lead-core rubber base isolation, higher-mode effects, plastic analysis, inelastic structures.

include friction pendulums, rubber bearings, and lead-core-rubber base isolators (LCR) [Dimizas and Koumousis 2005].

Disadvantages of base isolation systems include their vulnerability to strong pulse-type ground motions generated at near-fault zones [Kelly 1999]. The complementary damping provided by the base isolation may in certain cases induce energy into the higher modes of vibration and increase member deformations and accelerations of an isolated structure resulting in subsequent structural and nonstructural damages [Ramallo et al. 2002].

Examples of base isolated structures include the Los Angeles City Hall, Foothill Law, and the Justice Center in Los Angeles, California [Hart and Wong 2000]. The Bai-Ho Bridge that spans across the Gia-Nan canal in Taiwan utilizes an LCR isolation device [Shen et al. 2004], and the Yama-age Bridge in Japan employs a high-damping-rubber bearing dissipation system [Chaudhary et al. 2001]. The Marga-Marga Bridge in Vina del Mar, which is located in a high seismic risk area in Chile, is protected using high-damping rubber bearings [Boroschek et al. 2003]. Following the Great Hanshin/Awaji earthquake (also referred to as the Hyogo-Ken Nanbu, or Kobe earthquake) on January 17, 1995, the Benten Viaduct Highway Bridge in Kobe City, Japan was rebuilt in 18 months using LCR isolation [Yoshikawa et al. 2000].

Such catastrophes have motivated researchers to develop effective damage mitigation systems to protect various types of structures [Jangid 2004]. Base isolation has become a conventional method for protecting buildings and bridges from seismic events [Choi et al. 2006; Shen et al. 2004; Dicleli 2002]. Base isolation has been used to prevent brittle failure in piers [Hwang and Chiou 1996], to reduce the spectral accelerations in stiff piers, and to reduce the shear force at the bases of bridges [Soneji and Jangid 2006]. In short, it is generally considered a convenient alternative to typical bridge bearings [Chaudhary et al. 2001]. Tsopelas and Constantinou [1997] experimentally studied the use of sliding disc bearings and rubber restoring force devices to isolate bridge models under various types of ground motion excitations. The results showed that these devices resulted in significantly smaller responses than nonisolated bridges. Tsopelas et al. [1996] also performed analytical and experimental studies of elastoplastic isolated systems and concluded that these systems are vulnerable to shock-type seismic motions that result in large displacement demands. Over the last two decades, LCR isolators have been integrated into various buildings and bridges because of their large energy dissipation capability (via their large hysteresis region) and because of their attractive physical compactness [Choi et al. 2006].

In the current investigation, LCR isolators were applied in a benchmark study on the Highway 99 overpass at Second St. in Selma, CA in an effort to improve the performance of the overpass under a ground motion excitation. There are two physical components of LCR isolation that define its constituency. Several layers of rubber that help to support vertical loads while providing lateral flexibility, and the lead core component, which may be represented using the Bouc and Wen model [Wen 1976; Attard and Mignolet 2008], which has a significant physical advantage over bilinear models because of the additional energy dissipation capability that it provides [Ramallo et al. 2002].

The investigation herein focuses on five components. First, dynamic responses of an isolated stiff steel building are examined in order to validate the ability of the LCR isolator to protect structures from far field ground motions. Secondly, the ability of LCR isolators to reduce vibrations in stiff steel buildings subjected to near-field ground motions is analyzed. In this case, the near-field ground motion

is modeled as a nonstationary signal generated as modulated white noise filtered through a Kanai–Tajimi-like spectrum. Thirdly, the procedure is repeated by outfitting the LCR isolator in a building subjected to a component of the 1994 Northridge earthquake. Fourthly, the ability of LCR isolators to control the responses of an eight-story building responding at 'higher-mode effects' (HME) of vibration is analyzed under the ground motion of the El Centro ground acceleration record (S00E component) of the 1940 Imperial Valley Earthquake. Finally, a two-span bridge is modeled and analyzed using the El Centro motion.

Two parameters of the LCR isolator, which include the total yield force of the isolator and the pre-yield to post-yield stiffness ratio of the lead-core component, are parametrically varied in order to reduce the responses under the influence of HME or near-field or far-field ground motions and to determine the appropriate design of the LCR isolator. The steel sections of the shear frame buildings are defined using a highly nonlinear material model [Attard 2005], where the member stiffness is assumed to degrade smoothly following a constitutive rule that was developed to assess the behavior of kinematically strain-hardened materials under cyclic conditions. The results are compared to uncontrolled, or as-is, systems that would otherwise degrade highly nonlinearly [Attard 2005]. The yield force of the LCR system was represented using the Bouc and Wen model, whereas the bridge structure was linearly analyzed. The bridge was numerically modeled using site-plan information, and a suitable LCR isolator was designed. Responses of the isolated bridge subjected to the El Centro ground motion were evaluated and compared to those of the nonisolated bridge.

2. Equation of motion and the LCR model

The equation of motion of a structure integrated with LCR isolators and excited by a ground motion acceleration given as $\ddot{x}_g$ is

$$\boldsymbol{M}\ddot{\boldsymbol{x}} + \boldsymbol{C}\dot{\boldsymbol{x}} + \boldsymbol{K}\boldsymbol{x} + \boldsymbol{F}_R = \boldsymbol{\Gamma} f - \boldsymbol{M}\ddot{\boldsymbol{x}}_g. \tag{1}$$

Here $\boldsymbol{M}$ and $\boldsymbol{C}$ are the mass and damping matrices, respectively, where the mass matrix of the structure also includes a grade beam. The Caughey damping matrix [1960], $\boldsymbol{C}$, is assembled using all structural modal damping ratios. The displacement vector relative to the ground is defined as $\boldsymbol{x}(t)$. The stiffness matrix, $\boldsymbol{K}$, of the structure and the rubber component of the LCR isolator is elastic and provides a linear nonhysteretic component to the structure-LCR system until yielding occurs. At the point of yielding, the spring force in the post-yielded members remains constant (where $x_i(t) = x_{\text{yield},i}$, where $x_i(t)$ is the individual i-th member displacement, and $x_{\text{yield},i}$ is the respective yield displacement), and the subsequent hysteretic spring force, $\boldsymbol{F}_R$, is activated in those members where $x_i(t) > x_{\text{yield},i}$, including the LCR isolator. The nonlinear restoring force, $\boldsymbol{F}_R$, accounts for the material anisotropy in inelastic members that undergo cyclic deformations and that may be assumed to kinematically strain harden [Wu 2005; Elnashai and Izzuddin 1993]. The location vector $\boldsymbol{\Gamma}$ implies the position of the LCR isolator at the grade beam level, and f is a complementary hysteretic force of the lead core component of the LCR isolator of the form

$$f = ZQ_y, \tag{2}$$

where Q_y is the yielding force of the lead core and Z is a hysteretic component of the lead core used to smoothly transition the lead core's response between the elastic and post-yielded states. Tan and Huang [2000] used a bilinear hysteretic model to evaluate the behavior of LCR isolators in bridges, whereas in

the current investigation, this hysteretic component is represented using the Bouc and Wen model [Bouc 1968; Wen 1976; Attard and Mignolet 2008], the results of which have been shown to consistently match experimental data [Ramallo et al. 2002]. The Bouc and Wen model is given by

$$\dot{Z} = -\alpha\,|\dot{x}|\,Z^n - \beta\dot{x}\,|Z^n| + A\dot{x} \qquad \text{for odd values of } n, \tag{3}$$

where α, β, A, and n are shape parameters [Ramallo et al. 2002] and where

$$A = \frac{K_{\text{initial}}}{Q_{\text{total}}}, \qquad \alpha = \beta, \qquad A = \alpha + \beta. \tag{4}$$

Here K_{initial} is the initial stiffness of the LCR isolator and Q_{total} is the yield force of the LCR isolator which may be calculated as a percentage of a total weight of the structure. The equation of motion (1) is solved herein by marching in time from zero initial conditions by the Newmark Beta scheme assuming a linear change in the acceleration between time steps spread 0.02 s apart. The response simulations are made using an algorithm that was developed as part of this study called BISON (base isolated nonlinear time history analysis) that analyzes the local nonlinear plastic strain and global displacements of any damaged structural members using a nonlinear rule of kinematic strain hardening and formulates the LCR isolator force using the smooth Bouc and Wen model. Because the Bouc and Wen model is intrinsically hysteretic, the parameter n is chosen as 'one,' which allows a purely plastic region to exist once the lead core yields and enables a desirable smooth transition between the elastic and inelastic states. The LCR isolator is phenomenologically modeled as shown in Figure 1 and includes a slider that will open to indicate purely plastic behavior of the lead core after it yields ($n = 1$); the relative displacement of the two sides of the closed slider remains zero prior to yielding. Further, the displacement time histories of the lead core would 'drift' [Attard 2003; Attard and Mignolet 2005] using the Bouc and Wen model without inclusion of the nonhysteretic rubber components, and thus, these are consequently defined as $k_b x$ and $c_b \dot{x}$ and are included in the model of the LCR isolator as indicated by the equation

$$F_{LCR} = Z Q_y + k_b x + c_b \dot{x}. \tag{5}$$

The total force provided by the LCR isolator is F_{LCR}. The parameters k_b and c_b are the elastic stiffness and damping parameters of the rubber component where the nonhysteretic term, k_b, is included in the build-up of the matrix $\boldsymbol{K}$ in Equation (1). Once the lead core yields, the inelastic stiffness of the LCR isolator (lead core component + rubber component) is defined as k_b while the Bouc and Wen component of the LCR isolator provides a constant force equal to Q_y that is calculated at $x_i(t) = x_{\text{yield},i}$.

BISON calculates k_b by determining the stiffness of an additional so-called fictitious bottom story (in the case of a building) such that the fundamental period of the entire 'building + additional fictitious story' system is equal to 2.5 seconds [Ramallo et al. 2002]. This fictitious bottom story represents the LCR base isolator in the real structure. Caughey damping, which has been used in a previous study by [Attard 2007], is assumed to be 5% in each mode of vibration. The value of K_{initial} is calculated as

$$K_{\text{initial}} = B_{\text{ratio}} \times k_b, \tag{6}$$

where the parameters B_{ratio} and the LCR isolator yield force, Q_{total}, are LCR isolator design parameters that may be appropriately tuned to attain the desired response and controllability of the structure in question. In this study, stiff structures, structures subjected to near-field earthquakes, structures with and

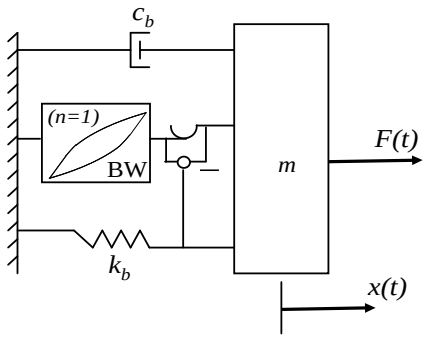

Figure 1. LCR isolator model assuming $n = 1$ in the Bouc and Wen model resulting in a sliding effect (perfectly plastic) after the lead core yields.

without HME, and a 2-span bridge are analyzed parametrically for various values of B_{ratio} and $\underline{Q_{\text{total}}}$. It has been suggested, however, that the following values be used for the parameter B_{ratio} depending on the peak ground acceleration (PGA) of the ground motion [Spencer et al. 2000]:

$$B_{\text{ratio}} = \begin{cases} 6 & \text{if PGA } \leq 0.35\,\text{g}, \\ 10 & \text{if PGA } > 0.35\,\text{g}. \end{cases} \tag{7}$$

3. Numerical examples: Five case studies

3.1. ***Two-story steel building subjected to the El Centro ground motion.*** The responses of a two-story steel building designed using LCR isolation were simulated using BISON. The building was excited using the El Centro ground motion with a time-step of 0.02 seconds. The shear frame is supported with a grade beam as shown in Figure 2, and the mass of each story, including the grade beam, is 0.5 kip·s^2/in. Each mode of vibration was assumed to have a damping ratio of 5% (assuming Caughey damping), and rock-like soil conditions were considered at the foundation level.

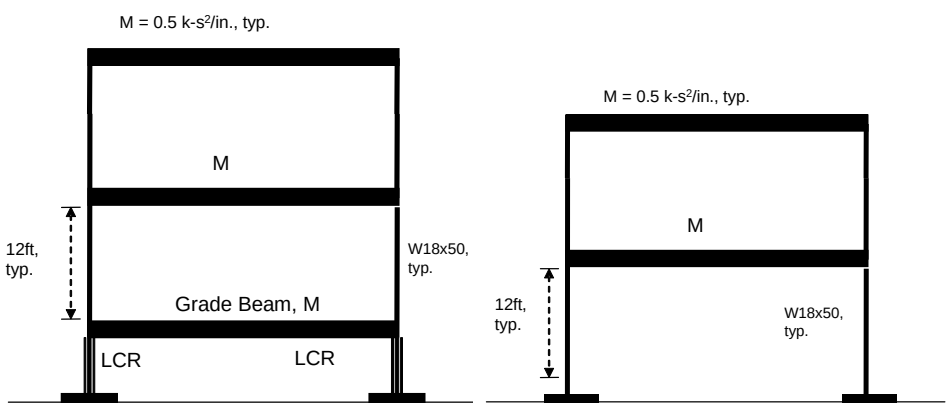

Figure 2. Two story stiff steel building: (a) passively controlled using LCR isolation supported under a grade beam; (b) uncontrolled ("as-is").

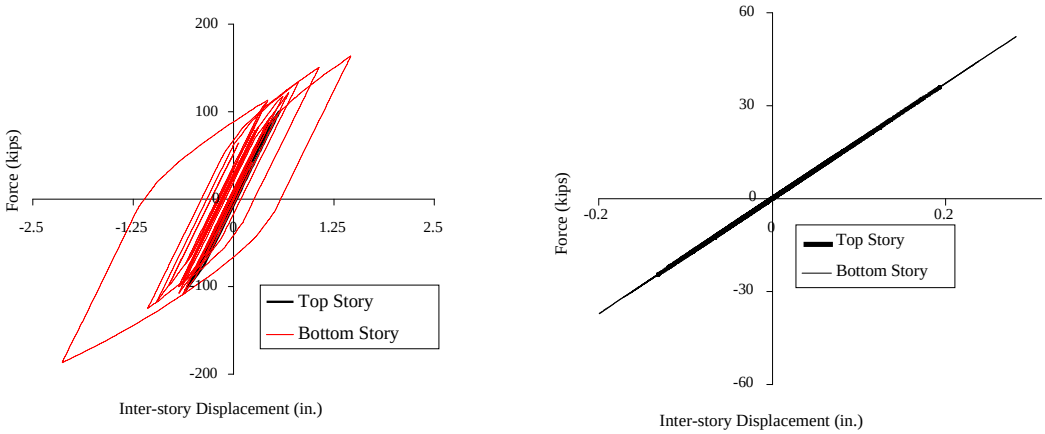

Figure 3. Hysteresis of a 2-story steel building subjected to the 1940 El Centro ground motion: (a) as-is frame [Attard 2005]; (b) isolated frame.

The frame was constructed using W18×50 steel sections that were 12 ft tall. The necessary post-yield stiffness of the LCR isolator (k_b) was calculated as 9.87 kip/in, whereby the fundamental period of the isolated structure equaled 2.5 seconds. The LCR isolator was designed to protect the building against moderate ground motions [Ramallo et al. 2002], having a PGA under 0.35 g's, with a corresponding B_{ratio} equal to 6; see (7). Skinner et al. [1993] and Spencer et al. [2000] suggest that the value of the yield force of the LCR isolator (Q_{total}) be 5% of the total weight of the structure.

The responses of the building in Figure 2 were marched in time from zero initial conditions using BISON. The force-displacement hysteresis of the as-is, or uncontrolled, frame is shown in Figure 3a, where the W18×50 members, especially those of the bottom story, experience significant damage. The nonlinear stiffness degradation model that was embedded in BISON and used to simulate the response time histories was derived following the one proposed by [Attard 2005]. The ability of the LCR isolator to reduce the displacement and velocity time histories is shown in Figures 3b and 4.

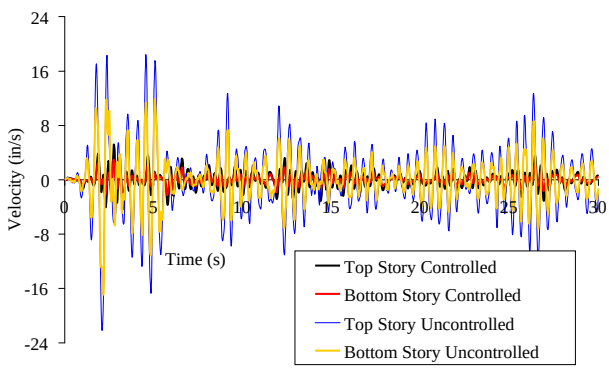

Figure 4. Velocity time histories of top and bottom stories of isolated and as-is frames subjected to the El Centro ground motion.

In Figure 3b, the maximum displacement of the frame with LCR isolation was reduced by over 50% with respect to the maximum displacement of the as-is building, implying that the higher frequencies of the ground motion were adequately filtered through the LCR isolator. Further, the structural members of the isolated frame did not exceed their yield limit (i.e., they remained elastic.). The LCR isolator was also able to significantly reduce the velocity time histories in the two-story building (Figure 4), which indicates that a significant amount of the input earthquake energy was dissipated, and that the acceleration responses were also reduced.

Finally, Figure 5a shows the smooth hysteresis of the LCR isolator, which was developed in BISON using the smooth Bouc and Wen model with the following parameters determined for Equation (3): $n = 1$, $A = 3.06$, $\gamma = 1.53$, $\beta = 1.53$.

The perfectly plastic hysteresis of the lead-core component is illustrated in Figure 5b, which shows the smooth transition between the elastic and plastic states ($n = 1$). Finally, Figure 5c shows that the rubber component remains elastic with a stiffness, k_b, equal to 9.87 kip/in, which is also the post-elastic stiffness of the LCR isolator shown in Figure 5a.

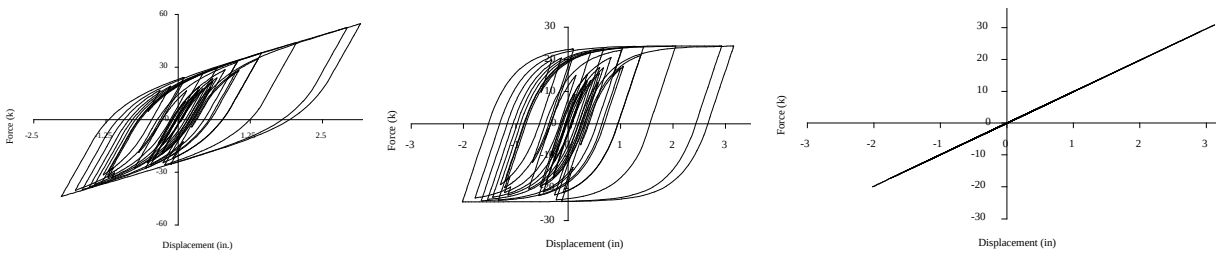

Figure 5. Hysteresis relationships of the (a) LCR isolator, (b) lead-core component using the Bouc and Wen model, and (c) rubber component using $k_b = 9.87$ kip/in.

3.2. ***Two-story building subjected to an artificial nonstationary excitation.*** In a second study, BISON was used to simulate the responses of the same two-story building in Figure 2 using a near-field ground excitation that was produced using a nonstationary signal generated as modulated Gaussian white noise filtered through a Kanai–Tajimi-like spectrum, $S_{gg}(\omega)$ equal to

$$S_{gg}(\omega) = G_o \frac{2\pi/\Delta t}{(\omega_g^2 - \omega^2)^2 + (2\xi_g \omega_g \omega)^2}, \tag{8}$$

where the ground intensity factor of the spectrum, G_o, is 0.126, and the ground frequency and damping terms, ω_g and ξ_g, are 15.6 radians/second and 0.6 [Clough and Penzien 1993]. It is possible to obtain the time histories of the ground motion (x_g) [Attard and Mignolet 2008], as the solution response to Equation (9) for a single-degree-of-freedom (single-DOF) ground system subjected to a white noise process, $\ddot{x}_{go}$, that has a spectral density of $G_o(2\pi/\Delta t)$, where

$$\ddot{x}_g + 2\xi_g \omega_g \dot{x}_g + \omega_g^2 x_g = -\ddot{x}_{go} \tag{9}$$

and

$$x_g(t) = \int_0^t h(t-\tau) F(\tau) d\tau \tag{10}$$

or

$$x_g(n\Delta t) = -\sum_{m=1}^{n} \frac{(\ddot{x}_{go}(m\Delta t) + \ddot{x}_{go}((m-1)\Delta t))}{2} h((n-m)\Delta t)\Delta t, \tag{11}$$

where $h(t-\tau)$ is the unit impulse response function, and n is the total number of time steps.

The k_b parameter equals to 9.87 kip/in in order to produce a fundamental period of 2.5 seconds to the isolated structure. The LCR isolator was redesigned with a new value of Q_{total} [Inaudi and Kelly 1993], following the ground excitation, $\ddot{x}_g$. Park and Otsuka [1999] suggested that the optimal range of Q_{total} be between 14% to 18% of the total weight of the building in order to achieve adequate seismic isolation and control building responses under severe ground motion. Spencer et al. [2000] further suggest that Q_{total} be selected between 13% to 17% of the total building weight and to select the stiffness ratio, B_{ratio}, to be approximately 10 in order to significantly reduce base drifts and moderate the acceleration responses for buildings subjected to severe ground motions. In this light, the LCR yield force, Q_{total}, was selected as 18% and $B_{\text{ratio}} = 10$ with due respect of the severe excitation described by (8) and (9). Figure 6 shows the force- displacement hysteresis of the as-is (uncontrolled) and LCR isolated buildings.

A comparison of the two figures indicates that the high energy content of the nonstationary excitation was not adequately dissipated via the lead core component of the LCR isolator. While the displacements of the top story were reduced as was the number of cycles, which indicated that the response remained linear for a longer period of time, the bottom story displacements were only marginally reduced as the structural member stiffness appears significantly nonlinear, which thus implies significant damage. An observation of the velocity time histories in Figure 7a — calculated relative to the LCR isolator velocities, which themselves are calculated relative to the ground — reveals that while the lead core component by definition increases the energy-dissipation capability of the base isolation system, the large velocities in particular indicate that LCR isolation is ineffective in reducing potential structural damages to the W18×50 structural members under this nonstationary excitation. It is in fact observed that the relative velocities of the bottom story of the LCR isolated frame exceed those of the as-is frame (red versus yellow in Figure 7a). In Figure 7b, the LCR isolation appears to have little impact on reducing the displacement

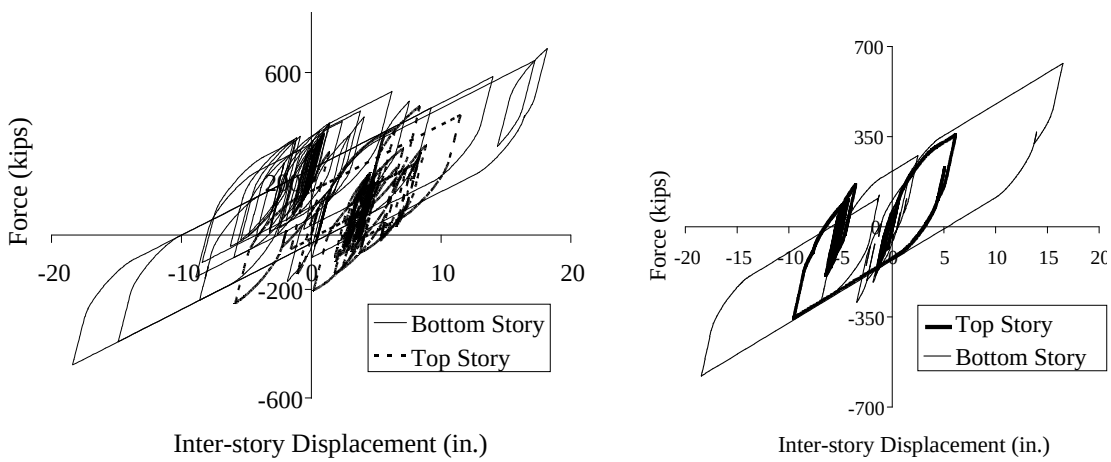

Figure 6. (a) As-is hysteresis. (b) LCR isolated hysteresis of 2-story steel building subjected to a nonstationary ground excitation.

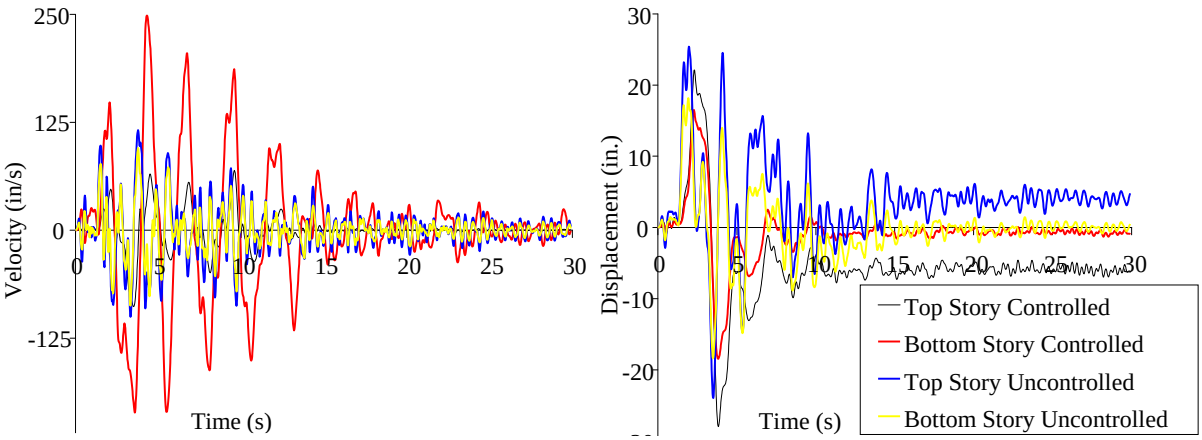

Figure 7. (a) Velocity and (b) displacement time histories of the Figure 2 frame under a nonstationary ground excitation having Kanai–Tajimi-like spectra.

time histories, but does appear to impose an out-of-phase component in the displacement time histories starting at about 6.5 seconds where the frequency abruptly reduces by a factor of about 2.

3.3. ***Two-story frame subjected to the Northridge (Pacoima Dam) motion.*** In a third investigation, the frame in Figure 2 was analyzed using the 1994 Northridge ground acceleration record (Pacoima Dam, Upper Left Abutment), which was a near-field ground motion having a PGA of 1.58 g's. According to (7), B_{ratio} should be equal to 10. Further, the value of Q_y is selected as 0.18. The results are shown in Figures 8 and 9, which indicates that LCR isolation is actually effective in reducing damages under this near-field excitation. Figure 8a shows the degree of structural damage to the W18×50 members in the as-is frame, where the damage was significantly reduced (Figure 8b), when LCR base isolation was integrated into the frame. The force-displacement hysteresis of the LCR isolation system is shown in Figure 8c, and a comparison of Figures 5a and 8c demonstrates the potential influence that pulse-type, near-field ground motions, such as the Northridge earthquake which was identifiable with historic structural and nonstructural damage, may have on the ability of an LCR isolation system to reduce structural responses, as indicated by the "nonstationary-like" hysteresis shown in Figure 8c. The comparison to Figure 5a, which had been determined using the El Centro earthquake, which was a far-field ground motion, shows that while the lead-core component is to some extent capable of dissipating the energy content of an incoming earthquake, the effects of which may be manifested in the velocity and acceleration time histories of the structural members, this may not necessarily be the case for pulse-type motions (9). In Figure 9, the story-level velocities are calculated relative to the LCR velocities. In this case, LCR isolation ineffectively attenuates the relative velocities, especially in the top story and especially later in the response-history when the velocities are actually shown to increase. This may be correlated to the 'nonstationary-like' nature of the LCR hysteresis, and in fact indicates that the velocities are most significantly reduced in either story when the LCR system does not reverse direction which occurs from 4.56 seconds to 5.36 seconds. This would then suggest that LCR isolation in this case precludes a structure from dissipating sufficient energy and reducing the structural velocities.

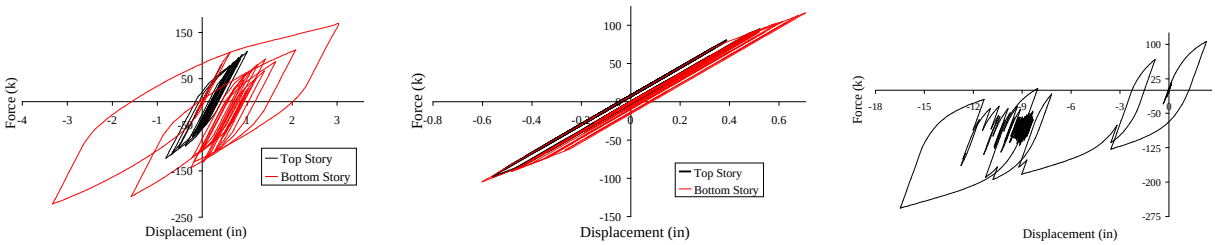

Figure 8. Responses of the LCR isolated 2-story steel frame (Northridge excitation) assuming $B_{\text{ratio}} = 10$: (a) as-is force-displacement hysteresis; (b) LCR-controlled hysteresis; (c) LCR hysteresis.

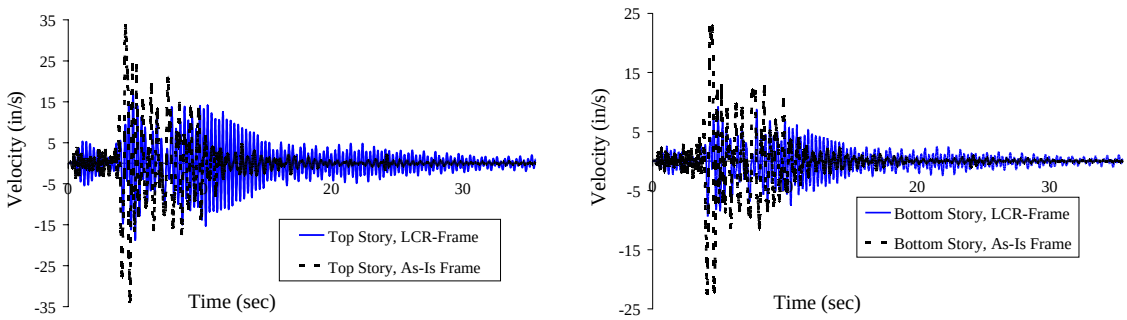

Figure 9. Responses of the LCR isolated 2-story steel frame (Northridge excitation) assuming $B_{\text{ratio}} = 10$: (a) top story velocity time histories; (b) bottom story velocity time histories.

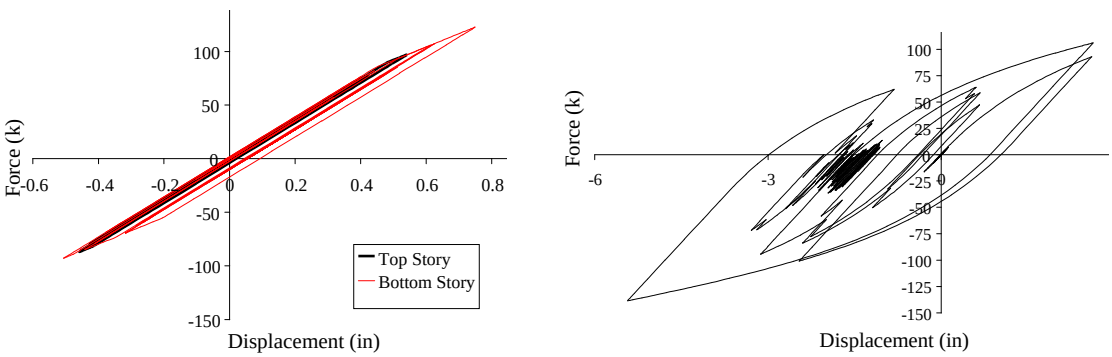

Figure 10. Responses of the LCR isolated 2-story steel frame (Northridge excitation) assuming $B_{\text{ratio}} = 6$: (a) force-displacement hysteresis; (b) LCR hysteresis.

In a follow-up to this analysis, a value of $B_{\text{ratio}} = 6$, while Q_y was held at 0.18, was used to design a new LCR system to try to mitigate the velocity differences between far-field and near-field excitations. The results are shown in Figures 10 and 11.

While the displacements were again effectively reduced, the structural velocity time histories (Figure 11) calculated relative to the LCR system, are also significantly smaller than those corresponding to

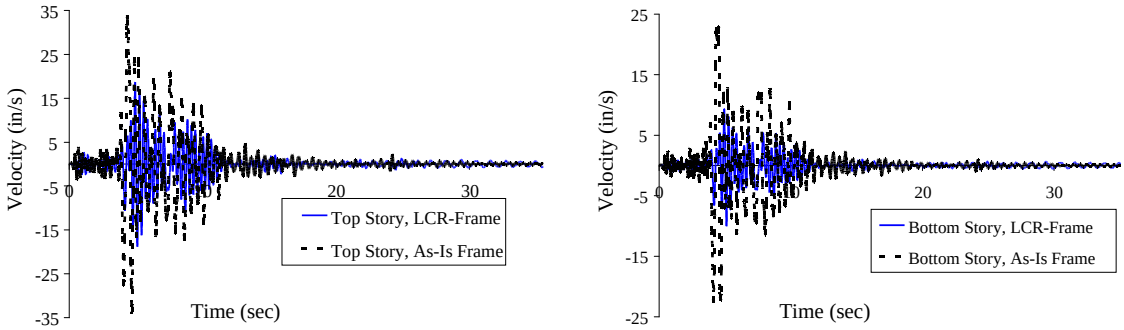

Figure 11. Responses of the LCR isolated 2-story steel frame (Northridge excitation) assuming $B_{\text{ratio}} = 6$: (c) top story velocity time histories; (d) bottom story velocity time histories.

Figure 9, where $B_{\text{ratio}} = 10$. What may be most telling in this comparison is the less nonstationary-like appearance of the LCR hysteresis in Figure 10b.

Finally, Figure 12 shows that the absolute acceleration time histories (structure + LCR isolator + ground accelerations) using a $B_{\text{ratio}} = 10$ versus $B_{\text{ratio}} = 6$. As was the case with the velocity time histories — see Figure 9 versus Figure 11 — a significant disparity exists between top story absolute accelerations for the suggested B_{ratio} of (7), versus the suggested value herein ($B_{\text{ratio}} = 6$). The current findings reveal that at least for near-field motions having large PGAs, LCR isolation systems should be designed using a softer elastic stiffness K_{initial} (i.e., $B_{\text{ratio}} = 6$), which affects energy dissipation of the lead-core component (A) — see (4) and (5) — and which finally results in a more stationary-like hysteresis (where the stiffness of the rubber component, k_b, remains unchanged).

3.4. ***Eight-story steel building responding with HME.*** In order to study the influence of HME on the design of an LCR isolation system, an eight story steel shear frame was designed having the properties as shown in Table 1. Each story was designed using W18×50 steel cross sections having a yield stress, σ_{yield}, of 36 ksi. The stiffness of the first story, k_1, was 9.54 times that of k_7; see Table 1. While the stiffness distribution over the height of the building (see 3rd column, Table 1) does not necessarily represent that of an actual building, it does ensure that the building will respond with HME in order to assess the

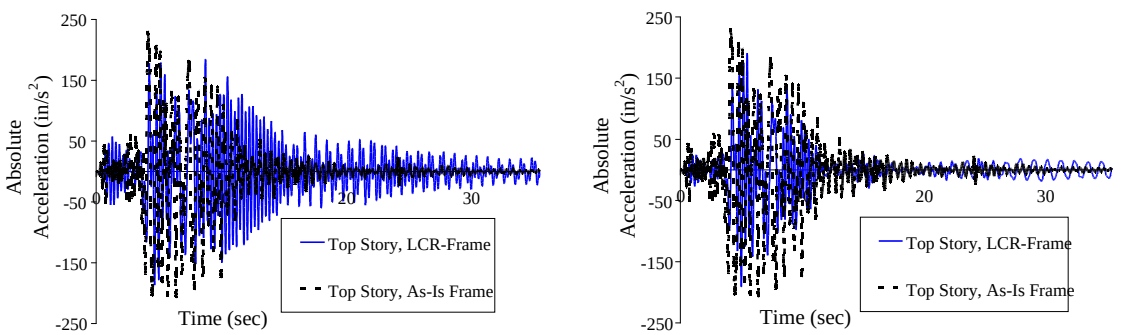

Figure 12. Comparison of absolute accelerations using (a) $B_{\text{ratio}} = 10$ and (b) $B_{\text{ratio}} = 6$.

story	mass (kip·s^2/in)	k_1/k_i	modal mass ratio
8	0.5	8	1.1% (8th mode)
7	0.5	9.54	5.5% (7th mode)
6	0.5	8	0.7% (6th mode)
5	0.5	5.35	0.6% (5th mode)
4	0.5	9.54	8.0% (4th mode)
3	0.5	3.38	8.2% (3rd mode)
2	0.5	1	9.4% (2nd mode)
1	0.5	1	66.4% (1st mode)

Table 1. Property distribution of an eight story stiff steel building with HME.

applicability of LCR isolation in HME-type systems. The modal mass ratio was 66.4%, which was less than 75% [Attard 2007], thus implying the presence of HME. If any of the W18×50 sections were to begin yielding, a smooth nonlinear model previously proposed by [Attard 2005] was assumed to govern the inelastic behavior, which was embedded in BISON. The damping ratio in each mode was assumed to be 5% following the previously mentioned Caughey model for damping.

The elastic stiffness of the LCR rubber component and the post-yield stiffness of the LCR (i.e., k_b) are calculated as 49.5 kip/in by BISON. The eight-story building is subjected to the El Centro ground motion. The value of B_{ratio} is 6, and Q_{total} is 5% of the total weight of the building as previously suggested [Skinner et al. 1993; Spencer et al. 2000].

The responses of the as-is and LCR-controlled buildings are shown in Figure 13. A comparison of the two figures reveals that LCR isolation significantly reduces the absolute maximum displacements (measured relative to the story immediately below, i.e., interstory displacements) on each story in the range of 7.29% to 33.06%, except for the 7th story which showed a slight increase of 0.23% in its interstory displacement, possibly due to the HME.

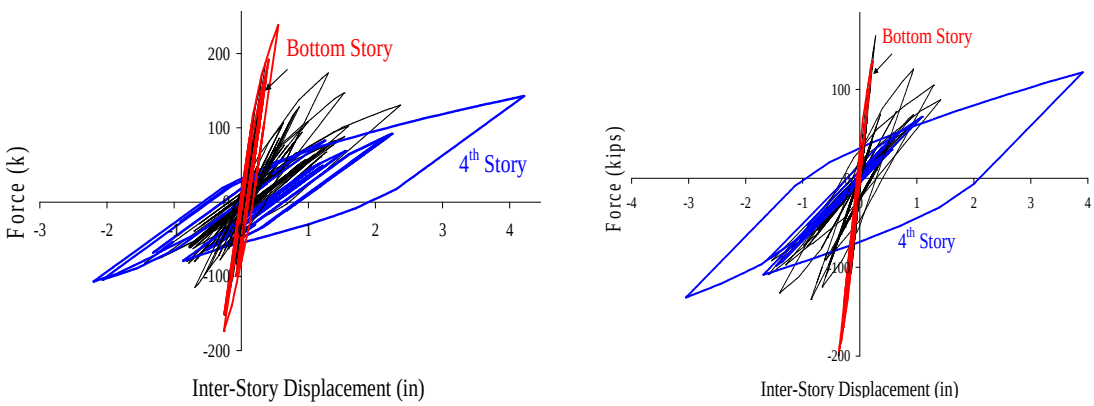

Figure 13. Eight-story steel building subjected to El Centro ground motion: (a) as-is hysteresis; (b) controlled hysteresis.

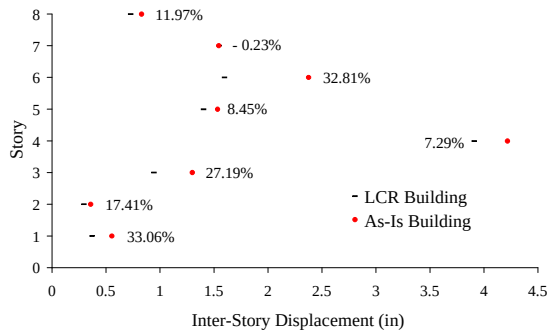

Figure 14. Distribution of interstory displacements between the as-is and LCR-controlled 8-story buildings (with HME); the percent error is shown to the side of each displacement pair per story.

The results are shown graphically in Figure 14, which display the percent error to the side of each interstory displacement. The negative error on story 7 indicates that the interstory displacement increased (0.23%) when LCR isolation was included. All other stories showed a substantial decrease. Note that the stiffness of the 4th story abruptly decreases following the first three 'stiff' stories. This sudden difference may be observed in Table 1 between k_1/k_3 and k_1/k_4, as the structure above the 3rd story in a sense 'decouples' from the first three stiff stories, thus enabling the first three stories to behave as a 'fixed-end' where stories 4–8 act as a 'cantilevered end.' The implication of this is that some dominant lower frequencies (HME exceeding 75%) remain unfiltered by the LCR isolator.

B_{ratio}	Q_{total}	8	7	6	5	4	3	2	1	GB
6	5%	−0.699	−1.501	−1.792	−1.558	3.837	1.016	−0.331	−0.413	−4.436
6	8%	−0.819	−1.734	2.199	−1.352	3.280	0.978	−1.041	0.853	−4.861
6	10%	−0.840	−1.875	−1.927	−1.522	−3.66	−1.078	−0.694	−0.537	−5.711
6	15%	−0.851	1.906	2.905	1.843	5.915	1.590	3.809	−2.459	6.645
6	18%	−0.897	2.696	2.870	1.587	3.388	1.650	1.450	1.355	3.541
10	5%	−0.758	−1.395	1.638	1.027	2.266	−0.815	−1.037	0.689	−3.927
10	8%	0.754	1.378	2.465	1.679	4.388	1.044	0.436	0.474	−10.07
10	10%	−0.891	1.511	2.874	2.168	5.345	1.332	9.817	−10.21	−10.28
10	15%	−0.918	1.821	2.376	1.537	5.063	1.269	0.868	−0.582	10.63
10	18%	−1.152	−2.384	2.210	−1.366	−3.028	3.077	−8.615	7.055	5.815
15	5%	−0.729	−1.677	−2.485	−2.424	−6.414	−3.111	−8.036	9.565	−7.122
15	8%	0.664	1.464	2.478	1.672	4.393	2.694	−5.221	3.863	−5.559
15	10%	−0.823	−1.736	1.741	1.156	−3.049	−1.291	0.642	−0.901	−8.254
15	18%	0.915	1.830	3.189	2.019	4.256	1.229	1.218	0.592	−29.762

Table 2. Maximum interstory displacement as a function of story number, pre-yield to post-yield stiffness ratio, and yield force of the LCR. The last column corresponds to the grade beam.

Table 2 shows the results of a comparative investigation of the influence of parameters B_{ratio} and Q_{total}, where the latter is the yield force of the LCR isolator and is given as a percentage of the total weight of the building, to correlate these parameters to the HME-induced responses, in this case for the 8-story building. The values of B_{ratio} were chosen as 6, 10, and 15, and for each B_{ratio}, the yield forces of the LCR isolator, Q_{total}, were varied between 0.05, 0.08, 0.10, 0.15, and 0.18 (except for $B_{\text{ratio}} = 15$, which did not include $Q_{\text{total}} = 0.15$) as the percentage of the total weight of the building. The responses were marched in BISON for 24 seconds (where the time between time steps, Δt, was assumed to be 0.02 seconds. The maximum displacements of each story in Table 2 include positive and negative signs of the calculated values to indicate the drift direction (right or left) of the maximum absolute displacement. The findings reveal that a combination of $B_{\text{ratio}} = 10$ and $Q_{\text{total}} = 0.05$ produces the smallest collection of interstory displacements and grade beam displacement. To validate these results, the use of $B_{\text{ratio}} = 6$ and $Q_{\text{total}} = 0.05$ will also result in reasonable interstory displacement time histories, although not as good as $B_{\text{ratio}} = 10$ and $Q_{\text{total}} = 0.05$, which is consistent with the findings of [Spencer et al. 2000].

A subsequent examination of the case where $B_{\text{ratio}} = 6$ shows that while an increase in Q_{total} will generally decrease the maximum interstory displacement on the 4th story (except for $Q_{\text{total}} = 0.15$) via a larger dissipative LCR hysteresis and because of the abrupt stiffness change on this floor, the unfiltered incoming lower frequencies tend to excite other pertinent HME resulting in an increase in the maximum displacements of the other stories, including the grade beam. These effects are more apparent as B_{ratio} increases. While a value of $Q_{\text{total}} = 0.18$ provides the best result for the grade beam displacement, this design value typically increases the maximum interstory displacements of many of the other stories. In the case of $B_{\text{ratio}} = 10$, the maximum displacements of many stories increase with an increase in Q_{total}, especially for $Q_{\text{total}} = 0.10$, where the maximum interstory displacements of the stiff 1st and 2nd stories abruptly increase. In this case, the inelastic stiffness of the LCR isolator, k_b, is relatively small and A in (4) and F_{LCR} in (5) are also small indicating that the "stiff" LCR isolator is unable to filter the ground motion frequencies associated with the stiff lower stories of the structure that result in a resonating effect in the response. In the case where $B_{\text{ratio}} = 15$, a decrease in Q_{total} (e.g., $Q_{\text{total}} = 0.05$ or 0.08) needs to be avoided in order to protect and not create a resonant-like response in the stiff lower stories. The results are illustrated in Figure 15, where Q_{total} as indicated is a percentage of the total weight of the building.

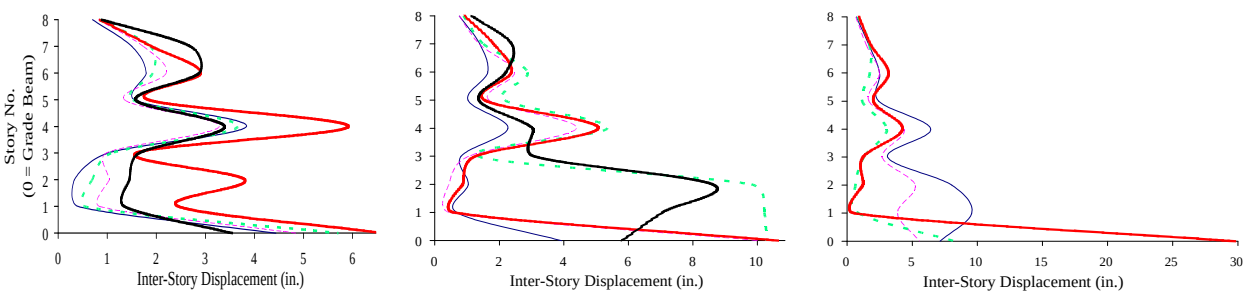

Figure 15. Maximum interstory displacement distributions measuring the impact of Q_{total} (%) on the LCR isolator design, for various B_{ratio} equal to 6 (left), 10 (middle) and 15 (right). The values of Q_{total} are 5 (thin black curve), 8 (magenta dashed curve), 10 (green dashed curve), 15 (red curve), 18 (thick black curve).

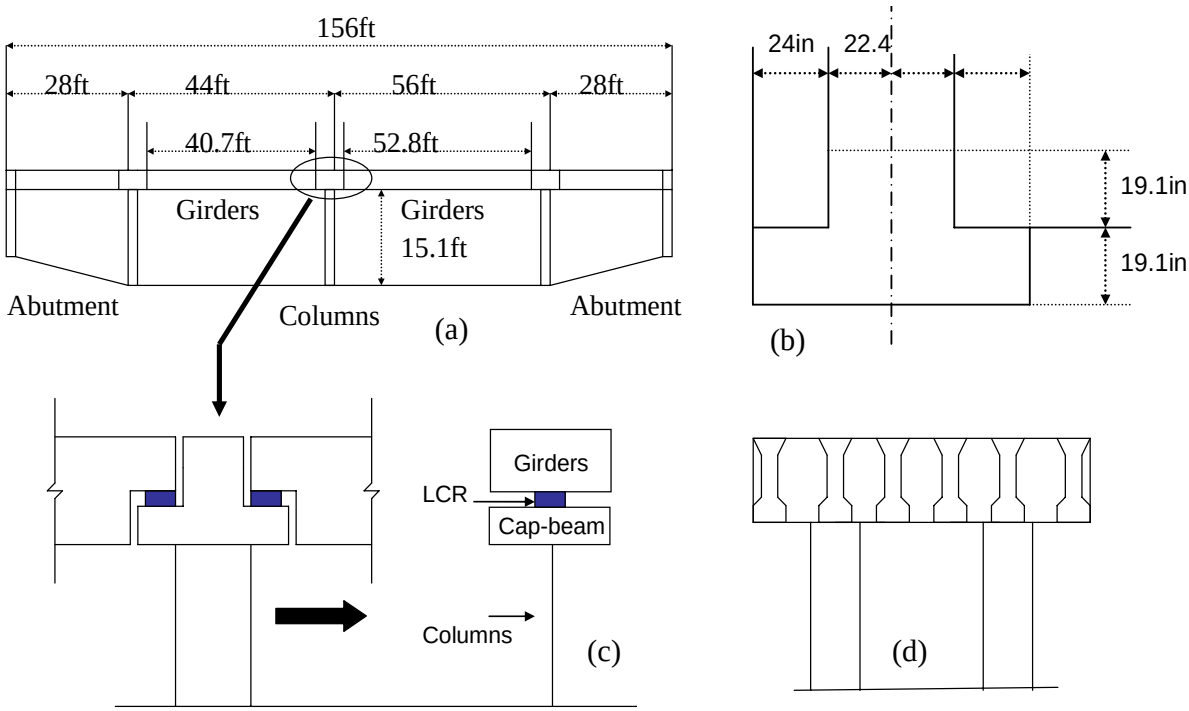

Figure 16. Elevation views of the two-span Highway 99 overpass used in the benchmark and LCR analyses: (a) overpass in the E-W direction; (b) cap girder supporting the LCR isolation pads; (c) 2-DOF model of the girder/cap-beam system; (d) overpass in the N-S direction of traffic.

3.5. ***Highway bridge protection using LCR isolation.*** In a final investigation, the highway 99 overpass across Second Street in Selma, CA was outfitted with LCR isolation using a lead core represented by the Bouc and Wen model. The bridge was numerically modeled following specifications of the California Department of Transportation. The LCR isolator was designed for the El Centro earthquake. Figure 16a shows an elevation view of the bridge, which spans 156 ft across two abutments. The bottom flanges of the supporting prestressed concrete girders are 15.1 ft above the ground and are supported by two center columns. An elevation view of the cap-beam is shown in Figure 16b; a detail of the girder-cap connection is shown in Figure 16c. Figure 16d shows the six-girder system together with the two columns aligned perpendicular to the flow of traffic in the North–South direction.

Using a unit weight of concrete of 150 lbs/ft^3 and a compressive concrete strength of 5,000 psi, the modulus of elasticity was calculated as 4,287 ksi, and the weight of the cap-beam was calculated as 89.51 kips. Each of the two columns supports half the weight of each of the two spans, where there are six girders per span; the weight of girders is 115.26 kips, and the diameter of each column is 3.74 ft. To study the effects of LCR base isolation on this bridge, LCR isolators were placed between the cap-beam and the girder to reduce the cap-beam displacement. The isolated bridge was modeled as a two-DOF system composed of the superstructure girders and the substructure cap-beam [Chaudhary et al. 2000; 2001]. The LCR isolator is situated between the cap-beam and the girders; see Figure 16c. The

		Girder		Cap-beam	
B_{ratio}	Q_{total}	displ. (in)	accel. (in/s^2)	displ. (in)	accel. (in/s^2)
6	5%	3.405	161.2	0.0617	163.3
6	10%	3.452	173.4	0.0612	163.3
6	15%	3.643	180.0	0.0604	163.3
10	5%	3.253	156.6	0.0604	163.3
10	10%	2.923	166.3	0.0596	163.2
10	15%	3.057	177.7	0.0589	163.2
15	5%	3.375	151.8	0.0598	163.3
15	10%	2.473	164.7	0.0591	163.2
15	15%	2.520	178.0	0.0584	163.2

Table 3. Maximum absolute displacements and accelerations of the girders and cap-beam (fixed-pin boundary conditions), for various values of B_{ratio}.

as-is system (having no LCR isolation) is modeled as a singe-DOF system having mass equal to that of the girders plus the cap-beam. Both systems were analyzed for a fixed-pinned boundary condition, per Caltrans' specs. The parameter B_{ratio} was varied between 6, 10, and 15, and Q_{total} was varied among 0.05, 0.10, 0.15 of the superstructure of the superstructure weight (girders) that was part of a parametric study used to design the LCR isolator for this bridge. For the assumed fixed-pinned boundary conditions, the post-yield stiffness of the LCR isolator was calculated as 1.89 kips/in using BISON that had resulted in a natural period of vibration for the system equal to 2.5 seconds after the lead-core had yielded. The maximum absolute displacements and accelerations of the girders and cap-beam are shown in Table 3, where Q_{total} is again given a percentage of the total weight of the bridge.

Table 3 shows that B_{ratio} has virtually no impact on the cap-beam accelerations and tends to result in a decrease in cap-beam displacements as it increases. The smallest absolute displacements of the girders (2.473 in) and cap-beam (0.0584 in) occur using $Q_{total} = 0.10$ and $B_{ratio} = 15$, and $Q_{total} = 0.15$ and $B_{ratio} = 15$, respectively. The girder accelerations (164.7 in/s^2) were smallest when $Q_{total} = 0.10$ and $B_{ratio} = 15$, and the cap-beam displacement (0.0591 in) was also adequately reduced using this combination in an ideal LCR design for a fixed-pinned connection. A comparison of the time history displacements and time history accelerations to those of the as-is case shows that the displacement demands on the cap-beam were reduced by 50% using LCR isolation (Figure 17a), and many of the time history accelerations of the cap-beam were also reduced, as indicated in Figure 17b. Figure 18 shows the hysteresis of the LCR isolator that had been modeled using the Bouc and Wen equations where $Q_{total} = 0.10$ and $B_{ratio} = 15$.

4. Conclusions

The ability of lead-core rubber base isolation (LCR) to reduce responses of buildings and bridges is investigated. Five case studies, including parametric analyses, of a stiff two-story structural steel building under (1) the El Centro (S00E component) ground motion, (2) a nonstationary signal, which was modeled

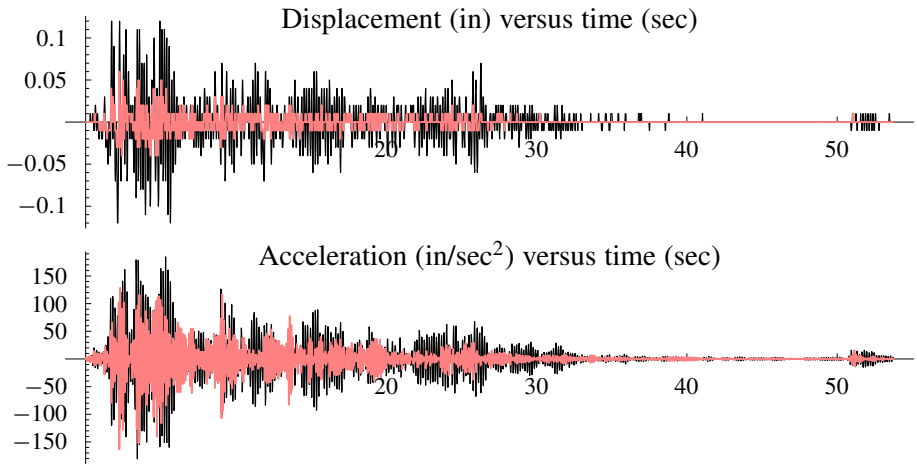

Figure 17. Response of the overpass bridge in Selma, CA with $B_{\text{ratio}} = 15$, $Q_{\text{total}} = 10$. Black curve: as-is response; superimposed lighter curve: LCR-isolated response.

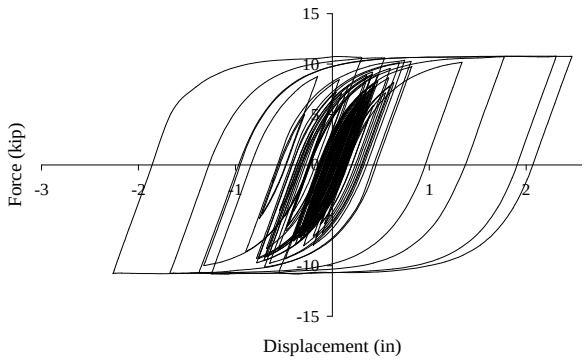

Figure 18. Response of the overpass bridge in Selma, CA with $B_{\text{ratio}} = 15$, $Q_{\text{total}} = 10$: LCR isolator's hysteresis.

as modulated Gaussian white noise passed through a Kanai–Tajimi filter, and (3) the Northridge (Pacoima Dam component) ground motion were analyzed. In addition, an eight-story steel building (4) exhibiting higher-mode effects was also studied, and a prestressed concrete bridge overpass (5) in Selma, CA were also examined using an in-house developed algorithm, called BISON (base isolation in nonlinear time history analysis). It appears that in all five cases, except under the action of the nonstationary signal input, parameters used to design the LCR isolator may be selected to very adequately reduce displacements, velocities, and accelerations by appropriately tuning the ratio of the LCR elastic-to-inelastic stiffness and the LCR yield force. Both parameters affect the LCR hysteresis, which was modeled using the Bouc and Wen model. In the cases where the LCR hysteresis had a stationary-like appearance, the responses were very adequately controlled, which was not the case under the nonstationary signal, where the high energy content associated with the low frequencies of the input appeared to not be adequately dissipated by the LCR isolator. However, in the four other cases, LCR isolation appears to be a very effective means of reducing seismic structural demands if appropriately tuned.

Acknowledgements

The writers gratefully acknowledge the support of this research by the California Department of Transportation (Caltrans) and especially the help of Mr. Mark Der Matoian, Mr. Robert James, and Mr. Alan Vong, and additionally for the support provided by Flatiron Constructors, Inc. (FCI) and Mr. Zeb Lemke.

References

[Attard 2003] T. L. Attard, *Modeling of higher-mode effects in various structures using a pushover analysis*, Ph.D. Thesis, Arizona State University, Tempe, AZ, 2003.

[Attard 2005] T. L. Attard, "Post-yield material nonlinearity: optimal homogeneous shear-frame sections and hysteretic behavior", *Int. J. Solids Struct.* **42**:21–22 (2005), 5656–5668.

[Attard 2007] T. L. Attard, "Controlling all interstory displacements in highly nonlinear steel building using optimal viscous damping", *J. Struct. Eng.* (*ASCE*) **133**:9 (2007), 1331–1340.

[Attard and Mignolet 2005] T. L. Attard and M. P. Mignolet, "Evolutionary model for random plastic analyses of shear-frame buildings using a detailed degradation model", pp. 533–540 in *Safety and reliability of engineering systems and structures: proceedings of the 9th International Conference on Structural Safety and Reliability* (*ICOSSAR 2005*) (Rome, 2005), edited by G. Augusti et al., Millpress, Rotterdam, 2005.

[Attard and Mignolet 2008] T. L. Attard and M. P. Mignolet, "Random plastic analysis using a constitutive model to predict the evolutionary stress-related responses and time passages to failure", *J. Eng. Mech.* (*ASCE*) **134**:10 (2008), 881–891.

[Boroschek et al. 2003] R. L. Boroschek, M. O. Moroni, and M. Sarrazin, "Dynamic characteristics of a long span seismic isolated bridge", *Eng. Struct.* **25**:12 (2003), 1479–1490.

[Bouc 1968] R. Bouc, "Forced vibration of a mechanical system with hysteresis", pp. 315 in *Proceedings of the Fourth Conference on Nonlinear Oscillations* (Prague, 1967), edited by J. Gonda and F. Jelínek, Academia Publishing, Prague, 1968. Abstract.

[Caughey 1960] T. K. Caughey, "Classical normal modes in damped linear dynamic systems", *J. Appl. Mech.* (*ASME*) **27**:2 (1960), 269–271.

[Chaudhary et al. 2000] M. T. A. Chaudhary, M. Abe, Y. Fujino, and J. Yoshida, "System identification of two base-isolated bridges using seismic records", *J. Struct. Eng.* (*ASCE*) **126**:10 (2000), 1187–1195.

[Chaudhary et al. 2001] M. T. A. Chaudhary, M. Abe, and Y. Fujino, "Performance evaluation of base-isolated Yama-agé bridge with high damping rubber bearings using recorded seismic data", *Eng. Struct.* **23**:8 (2001), 902–910.

[Choi et al. 2006] E. Choi, T. H. Nam, J. T. Oh, and B. S. Cho, "An isolation bearing for highway bridges using shape memory alloys", *Mater. Sci. Eng. A* **438–440** (2006), 1081–1084.

[Clough and Penzien 1993] R. Clough and J. Penzien, *Dynamics of structures*, 2nd ed., pp. 599–602, McGraw-Hill, New York, 1993.

[Dicleli 2002] M. Dicleli, "Seismic design of lifeline bridge using hybrid seismic isolation", *J. Bridge Eng.* **7**:2 (2002), 94–103.

[Dimizas and Koumousis 2005] P. C. Dimizas and V. K. Koumousis, "System identification of non-linear hysteretic systems with application to friction pendulum isolation systems", pp. 321–328 in *Proceedings of the 5th GRACM International Congress on Computational Mechanics* (*GRACM 05*) (Limassol, 2005), vol. 1, edited by G. Georgiou et al., Kantzilaris, Nicosia, 2005.

[Dolce et al. 2007] M. Dolce, D. Cardone, and G. Palermo, "Seismic isolation of bridges using isolation systems based on flat sliding bearings", *B. Earthq. Eng.* **5**:4 (2007), 491–509.

[Elnashai and Izzuddin 1993] A. S. Elnashai and B. A. Izzuddin, "Modelling of material non-linearities in steel structures subjected to transient dynamic loading", *Earthquake Eng. Struct. Dyn.* **22**:6 (1993), 509–532.

[Furukawa et al. 2005] T. Furukawa, M. Ito, K. Izawa, and M. N. Noori, "System identification of base-isolated building using seismic response data", *J. Eng. Mech.* (*ASCE*) **131**:3 (2005), 268–275.

[Hart and Wong 2000] C. G. Hart and K. Wong, *Structural dynamics for structural engineers*, Wiley, New York, 2000.

[Hwang and Chiou 1996] J. S. Hwang and J. M. Chiou, "An equivalent linear model of lead-rubber seismic isolation bearings", *Eng. Struct.* **18**:7 (1996), 528–536.

[Inaudi and Kelly 1993] J. A. Inaudi and J. M. Kelly, "Optimum damping in linear isolation system", *Earthquake Eng. Struct. Dyn.* **22**:7 (1993), 583–598.

[Jangid 2004] R. S. Jangid, "Seismic response of isolated bridges", *J. Bridge Eng.* **9**:2 (2004), 156–166.

[Kelly 1999] J. M. Kelly, "The role of damping in seismic isolation", *Earthquake Eng. Struct. Dyn.* **28**:1 (1999), 3–20.

[Kikuchi and Aiken 1997] M. Kikuchi and I. D. Aiken, "An analytical hysteresis model for elastomeric seismic isolation bearings", *Earthquake Eng. Struct. Dyn.* **26**:2 (1997), 215–231.

[Matsagar and Jangid 2004] V. A. Matsagar and R. S. Jangid, "Influence of isolator characteristics on the response of base-isolated structures", *Eng. Struct.* **26**:12 (2004), 1735–1749.

[Matsagar and Jangid 2008] V. A. Matsagar and R. S. Jangid, "Base isolation for seismic retrofitting of structures", *Pract. Period. Struct. Des. Constr.* **13**:4 (2008), 175–185.

[Park and Otsuka 1999] J.-G. Park and H. Otsuka, "Optimal yield level of bilinear seismic isolation devices", *Earthquake Eng. Struct. Dyn.* **28**:9 (1999), 941–955.

[Pozo et al. 2006] F. Pozo, F. Ikhouane, G. Pujol, and J. Rodellar, "Adaptive backstepping control of hysteretic base-isolated structures", *J. Vib. Control* **12**:4 (2006), 373–394.

[Ramallo et al. 2002] J. C. Ramallo, E. A. Johnson, and B. F. Spencer, Jr., "'Smart' base isolation systems", *J. Eng. Mech.* (*ASCE*) **128**:10 (2002), 1088–1099.

[Shen et al. 2004] J. Shen, M.-H. Tsai, K.-C. Chang, and G.-C. Lee, "Performance of a seismically isolated bridge under near-fault earthquake ground motions", *J. Struct. Eng.* (*ASCE*) **130**:6 (2004), 861–868.

[Skinner et al. 1993] R. I. Skinner, W. H. Robinson, and G. H. McVerry, *An introduction to seismic isolation*, Wiley, Chichester, 1993.

[Soneji and Jangid 2006] B. B. Soneji and R. S. Jangid, "Effectiveness of seismic isolation for cable-stayed bridges", *Int. J. Struct. Stabil. Dyn.* **6**:1 (2006), 77–96.

[Spencer et al. 2000] B. F. Spencer, Jr., E. A. Johnson, and J. C. Ramallo, "'Smart' isolation for seismic control", *Trans. Jpn. Soc. Mech. Eng. C* **43**:3 (2000), 704–711.

[Tan and Huang 2000] R. Y. Tan and M. C. Huang, "System identification of a bridge with lead-rubber bearings", *Comput. Struct.* **74**:3 (2000), 267–280.

[Tsopelas and Constantinou 1997] P. Tsopelas and M. C. Constantinou, "Study of elastoplastic bridge seismic isolation system", *J. Struct. Eng.* (*ASCE*) **123**:4 (1997), 489–498.

[Tsopelas et al. 1996] P. Tsopelas, M. C. Constantinou, S. Okamoto, S. Fujii, and D. Ozaki, "Experimental study of bridge seismic sliding isolation systems", *Eng. Struct.* **18**:4 (1996), 301–310.

[Wen 1976] Y. K. Wen, "Method for random vibration of hysteretic systems", *J. Eng. Mech.* (*ASCE*) **102**:2 (1976), 249–262.

[Wu 2005] H. C. Wu, *Continuum mechanics and plasticity*, Chapman and Hall/CRC Press, Boca Raton, FL, 2005.

[Yoshikawa et al. 2000] M. Yoshikawa, H. Hayashi, S. Kawakita, and M. Hayashida, "Construction of Benten Viaduct, rigid-frame bridge with seismic isolators at the foot of piers", *Cement Concrete Compos.* **22**:1 (2000), 39–46.

Received 4 Apr 2009. Accepted 16 May 2009.

THOMAS L. ATTARD: tattard@utk.edu
Department of Civil and Environmental Engineering, The University of Tennessee, 113 Perkins Hall, Knoxville, TN 37996-2010, United States

KITTINAN DHIRADHAMVIT: omchin@hotmail.com
Department of Civil and Environmental Engineering, The University of Tennessee, Estabrook Hall, Knoxville, TN 37996-2010, United States